ISME2010-3418

In-plane Vibrational Analysis of the Circularly Curved Carbon Nanotubes in Pasternak-Winkler Type Foundation

Payam Soltani[1,3], Mohammad Reza Saadati[2], Anoushiravan Farshidianfar[3]
[1]Department of Mechanical engineering, Islamic Azad University-Semnan branch, *p.soltani@semnaniau.ac.ir*
[2]Department of Mechanical engineering, Islamic Azad University-Semnan branch, *m.r.saadati@gmail.com*
[3]Department of Mechanical engineering, Ferdowsi University of Mashhad, *farshid@um.ac.ir*

Abstract
An interesting field in the nano science studies, is based on modeling and simulation of vibrating carbon nanotubes (CNTs) in an elastic medium to predict the natural frequencies and associated mechanical properties. Meanwhile, in all of these models, the nanotube was assumed to be perfectly straight. However, photomicrographs of nanocomposites indicate that CNTs may exhibit significant waviness. This research prepares a model based on the continuum mechanics to determine vibrational property of circularly curved carbon nanotube. Analysis of free vibration of a curved single-walled carbon nanotube (SWCNT) is accorded to the Timoshenko theory under general boundary conditions. Winkler and Pasternak foundation models are employed to simulate the interaction of the SWCNT with the surrounding elastic medium and the differential equations of the model are solved using generalized differential quadrature rule. The present study shows that the curvature of a CNT has a strong effect on modal frequencies, especially when the stiffness of the foundation and aspect ratio of CNT are relatively small.

Keywords: curved carbon nanotube, in-plane vibration, Timoshenko beam, general boundary condition, Winkler and Pasternak foundations

1. Introduction

Pursuant to superior mechanical, electrical and physical properties [1, 2], the number of publications on carbon nanotubes (CNTs) and related areas have grown quickly since CNT discovered by Ijima in 1991[3]. Because of high strength and stiffness of CNTs, they are widely used as reinforced phase in composite materials [4]. Since molecular dynamic simulations are difficult for large scales, continuum mechanics are applied to study the elastic and vibrational behavior of CNTs [5-7]. In all of these cases, the simulated model of CNTs was straight. However, photomicrographs of nanocomposites show that CNTs may exhibit significant waviness in nanocomposites [8]. Recently several studies have been done on the effects of waviness on characteristics of CNTs. Pantano and Boyce [9] studied the effect of the characteristic wavelike or wrinkles on the bending mode of CNT under considering the geometric nonlinearity and showed the phenomenon that the bending stiffness of CNT decrease with the increase of the diameter of CNT. According to Fisher et al. [10-11], the effect of elastic moduli of CNT-reinforced polymer composites cannot be ignored. F.N. Mayoof and M.A. Hawwa [12], indicated Chaotic behavior of a curved SWCNT under harmonic excitation. However, it seems that no work has been thoroughly done on the effects of waviness on the vibration characteristics of CNTs [13].

Before the above studies, several researches about vibration of arched beams have been started since several decades ago. The studies which are about in-Plane vibration are based on Bernoulli-Euler and Timoshenko beam theories. The Bernoulli-Euler theory neglects the effect of rotary inertia and shear deformation. Significant difference in natural frequencies can be seen while a short beam is solved by Timoshenko theory in compare with Bernoulli-Euler. Timoshenko theory has been employed using various boundary conditions, elastic foundations, etc. and scientific solutions. In-plane vibration based on curved Timoshenko beam theory has been carried out in several studies [15-20].

This paper has five main objectives: (1) to present the differential equations for the in-plane free vibration of linearly elastic curved SWCNT; (2) to include the effect of variable curvatures with the different the opening angles, slenderness ratios and curvature radiuses; (3) to include effects of rotary inertia and shear deformation; (4) to present solutions for the general boundary conditions; and (5) to exhibit elastic model for the nanocomposites with Winkler and Pasternak foundations. GDQR formulation has been applied to solve the problem numerically. The fundamental frequencies are calculated with general boundary conditions. In addition, effects of nanotube curvature and elastic medium on the natural frequencies of a curved SWCNT has been calculated and discussed. The results show that the curvature of a CNT, the boundary conditions and the mechanical properties of the foundation have strong effect on resonant frequencies, especially when the aspect ratio of CNT is relatively large. Additionally, the effect of the aspect ratio, Pasternak and Winkler constants, and the opening angle on the vibrational characteristics of the model has been widely discussed.

2. Governing equations

As shown in Figure 1, the circularly curved SWCNT is modeled on Winkler-type and Pasternak-type foundation. Every point on the SWCNT is defined by the angle θ, measured from the left end. The system consists of a uniformly curved SWCNT of radius R, average diameter of SWCNT d_{ave}, length L and the opening angle is θ_0. Denote the displacements as u and w corresponding to the radial and tangential displacements, respectively.

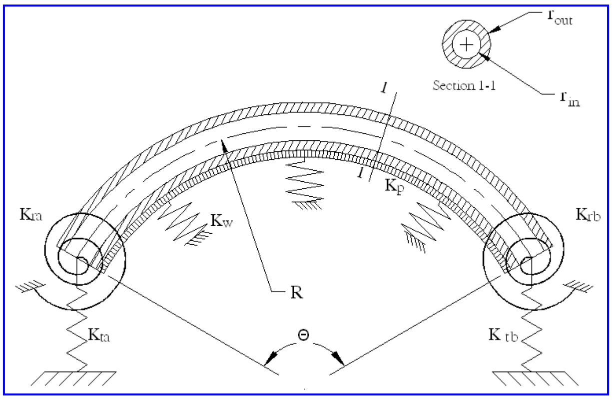

Figure 1: circularly curved SWCNT on elastic medium with the general boundary condition.

Using Timoshenko beam theory, both rotary inertia and shear deformation are taken into account. The differential governing equations for the in-plane vibration of SWCNT on Winkler-type and Pasternak-type models are expressed by [16, 18].

$$(\frac{\kappa}{2(1+\nu)}+K_3)\frac{u''}{R\theta_0^2}-(1-\lambda^2\frac{1+K^2}{S^2}+K_4)\frac{u}{R}-\frac{\kappa}{2(1+\nu)}\frac{\psi'}{\theta_0}+(1+\frac{\kappa}{2(1+\nu)})\frac{w'}{R\theta_0}=0 \tag{1}$$

$$\frac{\kappa}{2(1+\nu)}\frac{u'}{R\theta_0}+K^2\frac{\psi'}{\theta_0^2}-(\frac{\kappa}{2(1+\nu)}-\lambda^2\frac{K_2^2}{S^2})\psi+(\frac{\kappa}{2(1+\nu)}+\lambda^2\frac{K_1^2}{S^2})\frac{w}{R}=0 \tag{2}$$

$$(1+\frac{\kappa}{2(1+\nu)})\frac{u'}{R\theta_0}-(\frac{\kappa}{2(1+\nu)}+\lambda^2\frac{K_1^2}{S^2})\psi-\frac{w'}{R\theta_0^2}+(\frac{\kappa}{2(1+\nu)}-\lambda^2\frac{1+\kappa^2}{S^2})\frac{w}{R}=0 \tag{3}$$

Where κ is shear coefficient factor on its cross-sectional shape, ν is the Poisson's ratio of the SWCNT and ψ is the slope of the deflection of the curved nanotube due to pure bending. λ and S are two dimensionless variables have been introduced as follows:

$$S=\frac{4}{\theta_0}\times\frac{L}{d_{ave}}, \qquad \lambda^2=\frac{\rho AR^4\omega^2}{EI} \tag{4}$$

λ is a dimensionless frequency parameter and S is the slenderness ratio of the SWCNT. Where A is the cross-sectional area, ρ is the density, ω is the natural frequency, I is the moment of inertias of cross-section about principal axes and E is the Young's modulus of the curved SWCNT. In Eqs. (1-3), the quantities K^2, K_1^2, K_2^2, K_3 and K_4 are the dimensionless parameter defined as:

$$K^2=(\frac{d_{ave}}{4R})^2,\quad K_1^2=K^2(1+K^2),\quad K_2^2=K^2(1+4K^2+K^4) \tag{5}$$

$$K_3=\frac{K_P}{EA}, K_4=\frac{K_w R^2}{EA} \tag{6}$$

In which K_P is the shear modulus parameter due to the Pasternak foundation and K_w is the Winkler modulus parameter.

In the boundary conditions, the shear force F, the tensile force P and the bending moment M could be expressed in terms of amplitude u and w [25] and were given as:

$$F=\frac{\kappa AG}{R}\left[\frac{\partial u}{\partial\theta}+w-R\psi\right] \tag{7}$$

$$P=\frac{EA}{R}\left[-u+\frac{\partial w}{\partial\theta}\right] \tag{8}$$

$$M=EARK^2\frac{\partial\psi}{\partial\theta} \tag{9}$$

Each end of the arch was supported by two separate springs, the linearly elastic translational K_t and rotational K_r springs (Figure 1). At the left end ($\theta=0$), the spring constants are ($K_t=K_{ta}$) and ($K_r=K_{ra}$) and at the right end ($\theta=\theta_0$), the spring constants are ($K_t=K_{tb}$) and ($K_r=K_{rb}$).Therefore, the shear force F, the tensile force P and the bending moment M corresponding to K_t and K_r with deflection u and w and rotation θ could be expressed as

$$F=K_t u\cos\frac{\theta}{2} \tag{10}$$

$$P=K_t w\sin\frac{\theta}{2} \tag{11}$$

$$M=K_r\psi \tag{12}$$

Combining Eqs.(7-9) with Eqs.(10-12) give the boundary equations as follows

$$\frac{\kappa AG}{R}\left[\frac{\partial u}{\partial\theta}+w-R\psi\right]-K_t u\cos\frac{\theta}{2}=0 \tag{13}$$

$$\frac{EA}{R}\left[-u+\frac{\partial w}{\partial\theta}\right]-K_t w\sin\frac{\theta}{2}=0 \tag{14}$$

$$EARK^2\frac{\partial\psi}{\partial\theta}-K_r\psi=0 \tag{15}$$

Nanotubes in nanocomposite materials may undergo different and general conditions in which it may not be a standard boundary conditions but between of them. Thus, general boundary conditions support all probable boundary conditions. Several standard boundary conditions based on the boundary stiffness of this model are shown in table 1.

3. The generalized differential quadrature rule

Differential Quadrature method (DQM) is a numerical method for evaluating derivatives of a sufficiently smooth function, proposed by Bellman and Casti in 1971. The basic idea of DQM comes from Gauss Quadrature, a useful numerical integration. This method approach has been extensively used to solve various problems in different fields of science.

Table1. Standard boundary conditions based on boundary stiffness.

Standard Boundary conditions	Stiffness			
	K_{ta}	K_{tb}	K_{ra}	K_{rb}
Pinned-Pinned	∞	0	∞	0
Fixed- Fixed	∞	∞	∞	∞
Free- Free	0	0	0	0
Fixed- Pinned	∞	∞	∞	0
Fixed- Free	∞	∞	0	0
Fixed-Slide	∞	∞	0	∞
Pinned- Free	∞	0	0	0

New achievement in the DQM causes the development of a generalized differential quadrature rule (GDQR). The GDQR can be applied to any high-order differential equations without using the conventional δ -point technique. The GDQR has been shown to be a powerful contender in solving initial and boundary value problems. Suppose a function $\psi(x)$ is governed by a differential equation, is constrained by one or more conditions at any individual point. The solution domain is divided by points $x_i (i = 1,2,..., N)$ that include all the points with given conditions. If n_i conditions (equations) are to be satisfied at point x_i, the GDQR is expressed as follows:

$$\frac{d^r\psi(x_i)}{dx^r} = \sum_{j=1}^{N}\sum_{l=0}^{n_j-1} C_{ijl}^{(r)}\psi_j^{(1)} = \sum_{K=1}^{M} C_{ik}^{(r)} U_k \quad (i = 1,2,..., N) \quad (16)$$

Where $C_{ik}^{(r)}$ (which is a convenient expression of $C_{ijl}^{(r)}$) is the weighting coefficient corresponding to the r th order derivative at point x_i and $M = \sum_{i=1}^{N} n_i$ is the number of the total independent variables U_k, which is expressed in series as

$$\{U\}^T = \{U_1, U_2,\dots, U_k,\dots, U_m\}^T = \{\psi_1^{(0)}, \psi_1^{(1)},\dots, \psi_1^{(n_i-1)},\dots, \psi_N^{(0)}, \psi_N^{(1)},\dots, \psi_N^{(n_N-1)}\}^T \quad (17)$$

Where $\psi_i^{(0)} = \psi(x_i) = \psi_i$ is the function value, $\psi_i^{(k)} = \psi^{(k)}(x_i) \quad (k = 1,2,..., n_i - 1)$ its k th order derivatives. The weighting coefficients for r th order derivative are given by recurrence relations in general form as [21]:

$$C_{ij}^{(1)} = \frac{M^{(1)}(x_i)}{(x_i - x_j)M^{(1)}(x_j)} \quad for \quad i \neq j \quad and \quad i, j = 1,2,\dots,N \quad (18)$$

and

$$C_{ij}^{(1)} = C_{ii}^{(1)} = -\sum_{k=1, i\neq k}^{N} C_{ik}^{(1)} \quad for \quad i, j = 1,2,..., N \quad (19)$$

For the higher order derivatives, the weighting coefficients are obtained by using the following recurrence relationship:

$$C_{ij}^{(r)} = r(C_{ii}^{(r-1)}C_{ij}^{(1)} - \frac{C_{ij}^{(r-1)}}{x_i - x_j} \quad for \quad i \neq j; \quad r = 2,3,\dots N-1; \quad i, j = 1,2,\dots,N \quad (20)$$

and when $i = j$

$$C_{ij}^{(r)} = C_{ii}^{(r)} = -\sum_{k=1, i\neq k}^{N} C_{ik}^{(r)} \quad for \quad r = 2,3,\dots,N-1 \quad (21)$$

The term $M(x_i)$ is defined as

$$M(x_i) = \prod_{j=1}^{N}(x - x_j) \quad (22)$$

Another important point for successful application of the GDQR is how to distribute the grid points. In fact, the accuracy of this method is usually sensitive to the grid point distribution. The optimal grid point distribution depends on the order of derivatives in the boundary condition and the number of grid points used. The nonuniform grid points are better known as Chebyshev–Gauss–Lobatto points (C–G)[22]:

$$x_i = \frac{1}{2}\left[1 - cos(\frac{i-1}{N-1}\Pi)\right] for \quad i = 1,2,\dots,N. \quad (23)$$

4. Applying the GDQR to the curved SWCNT vibration

The GDQR is used to formulate solutions to Eqs. (1) - (3).

$$(\frac{\kappa}{2(1+v)} + K_3)\frac{1}{R\theta_0^2}\sum_{j=1}^{N} C_{ij}^{(2)}u_j - (1 - \lambda^2\frac{1+K^2}{S^2} + K_4)\frac{u_i}{R} - \frac{\kappa}{2(1+v)}\frac{1}{\theta_0}\sum_{j=1}^{N} C_{ij}^{(1)}\psi_j + (1 + \frac{\kappa}{2(1+v)})\frac{1}{R\theta_0}\sum_{j=1}^{N} C_{ij}^{(1)}w_j = 0 \quad (24)$$

$$\frac{\kappa}{2(1+v)}\frac{1}{R\theta_0}\sum_{j=1}^{N} C_{ij}^{(1)}u_j + K^2\frac{1}{\theta_0^2}\sum_{j=1}^{N} C_{ij}^{(2)}\psi_j - (\frac{\kappa}{2(1+v)} - \lambda^2\frac{K_2^2}{S^2})\psi_i + (\frac{\kappa}{2(1+v)} + \lambda^2\frac{K_1^2}{S^2})\frac{w_i}{R} = 0 \quad (25)$$

$$(1 + \frac{\kappa}{2(1+v)})\frac{1}{R\theta_0}\sum_{j=1}^{N} C_{ij}^{(1)}u_j - (\frac{\kappa}{2(1+v)} + \lambda^2\frac{K_1^2}{S^2})\psi_i - \frac{1}{R\theta_0^2}\sum_{j=1}^{N} C_{ij}^{(2)}w_j + (\frac{\kappa}{2(1+v)} - \lambda^2\frac{1+\kappa^2}{S^2})\frac{w_i}{R} = 0 \quad (26)$$

Where $C_{ij}^{(1)}$ and $C_{ij}^{(2)}$ are the weighting coefficients along the dimensionless axis for the first and second derivatives, respectively. Similarly, the GDQR is applied to the boundary conditions. Eqs. (13-15) are written according to Eq. (16) as follows:

$$\frac{\kappa AG}{R}\left[u_i^{(1)}+w_i-R\psi_i\right]-K_t u_i \cos\frac{\theta}{2}=0 \qquad (27)$$

$$\frac{EA}{R}\left[-u_i+w_i^{(1)}\right]-K_t w_i \sin\frac{\theta}{2}=0 \qquad (28)$$

$$EARK^2\psi_i^{(1)}-K_r\psi_i=0 \qquad (29)$$

By using the GDQR, domain equations and boundary conditions for in-plane vibrations of a circular SWCNT can be transformed to an assembled form given by

$$\begin{bmatrix}[S_{bb}] & [S_{bd}]\\ [S_{db}] & [S_{dd}]\end{bmatrix}\begin{Bmatrix}\{U_b\}\\ \{U_d\}\end{Bmatrix}=\begin{Bmatrix}\{0\}\\ \lambda^2\{U_d\}\end{Bmatrix} \qquad (30)$$

Where the subscript b denotes elements associated with the boundary points (at the two ends of the curved SWCNT) while d the remainder. By matrix subtracting and manipulation, one obtains a standard eigenvalue equation:

$$[S]\{U_d\}=\lambda^2\{U_d\} \qquad (31)$$

in which

$$[S]=[S_{dd}]-[S_{db}][S_{bb}]^{-1}[S_{bd}] \qquad (32)$$

5. Numerical results and comparison

Based on the above equations, the resonant frequencies of the in-plane vibration of a circularly curved SWCNT are derived using GDQR. By considering a SWCNT with an inner diameter 0.7 nm and an outer diameter 1.4 nm. It is assumed that the Young's modulus, Poisson's ratio and mass density of SWCNT are $E=1Tpa$, $\nu=0.25$ and $\rho=2.3\,{gr}/{cm^3}$ respectively also the shear correction factor κ is taken to be 0.82 [23].

Firstly, natural frequencies are found by using generalized differential quadrature rule (GDQR) and given in table 2 for in-plane vibrations of curved SWCNT. SWCNT is assumed to be circularly curved with the clamped condition at both ends, the opening angle is equal to 180° and the stiffness coefficients of Winkler and Pasternak are zero. Natural frequencies are given for the first three modes (n=1, 2and 3) and for the various amounts of aspect ratios ${l}/{d}$.

Table2. Natural frequency of in-plane vibration for circular curved SWCNT

L/d	n	f (THZ)
10	1	0.44812
	2	0.84311
	3	1.46228
20	1	0.12304
	2	0.25933
	3	0.47326
100	1	0.00509
	2	0.01118
	3	0.02075

The circularly curved SWCNT with various opening angles and stiffness parameters $K_w=K_p=0$ has been studied under clamped-clamped conditions for many mode numbers and Figures 2 and 3 compared these results for a curved SWCNT with small and large aspect ratios, respectively. It is observed from these figures that the natural frequency is sensitive to increasing the aspect ratios l/d. Meanwhile, maximum variations in frequencies occur when the opening angel decreases while slenderness ratio increases.

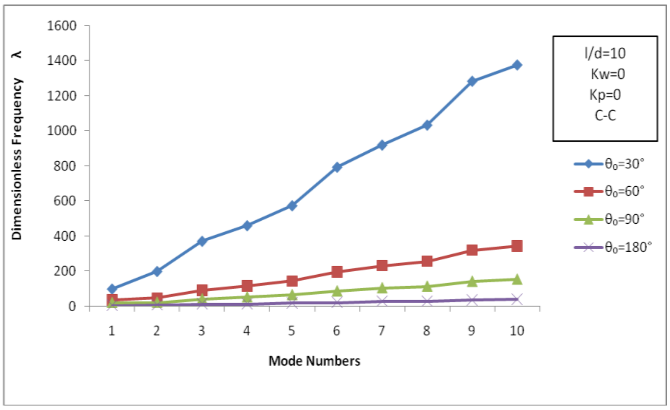

Figure 2: Fundamental frequency of in-plane vibration of short curved SWCNT against mode numbers for various opening angles.

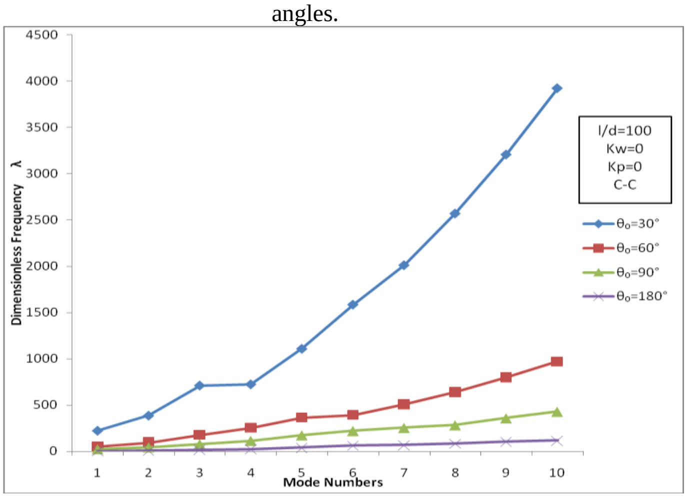

Figure 3: Fundamental frequency of in-plane vibration of long curved SWCNT against mode numbers for various opening angles.

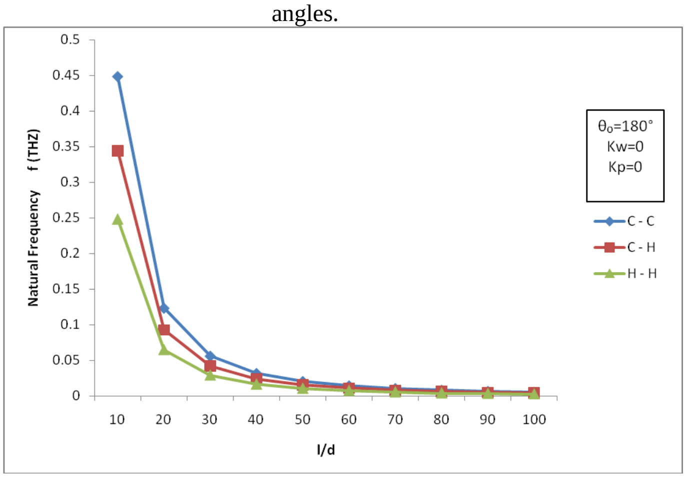

Figure 4: First natural frequency of in-plane vibration of curved SWCNT against the different aspect ratios for various end conditions.

The effect of the aspect ratio on the first natural frequency of in-plane vibration for semi circular SWCNT ($\theta_0=180^{\circ}$) under three standard boundary conditions is shown in figure 4. In addition, in this figure, the Pasternak parameter K_P and the Winkler parameter K_W are equal to zero. As shown in this figure the natural frequencies of each standard boundary condition are converged to each other for long slenderness ratios.

The effect of the Winkler stiffness on a semi circular SWCNT under clamped-clamped condition without Pasternak shear modulus effects (K_P =0) is presented in figure 5. The resonant frequencies increases considerably while the aspect ratio *l/d* and Winkler parameter K_W increase. In this case, with increasing the bending stiffness of SWCNT due to the Winkler stiffness, the variation on the natural frequencies rises and this effect is obviously clear for the stiffer elastic mediums (say $K_W > 10^8$) .

Efficacy of Pasternak parameter K_P on a curved SWCNT under clamped-clamped condition is shown in figure 6 when Winkler constant is neglected. Like the pervious case, the resonant frequency increases with increasing the Pasternak shear stiffness K_P and aspect ratios *l/d*. However, the gradients of the curves are linear respect to the nonlinear gradient of the curves in figure 5.

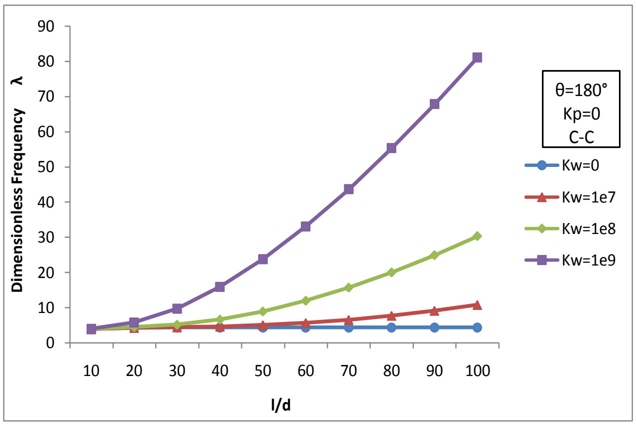

Figure 5: The effect of the Winkler foundation parameter with various slenderness ratios on the dimensionless frequencies of a circular SWCNT.

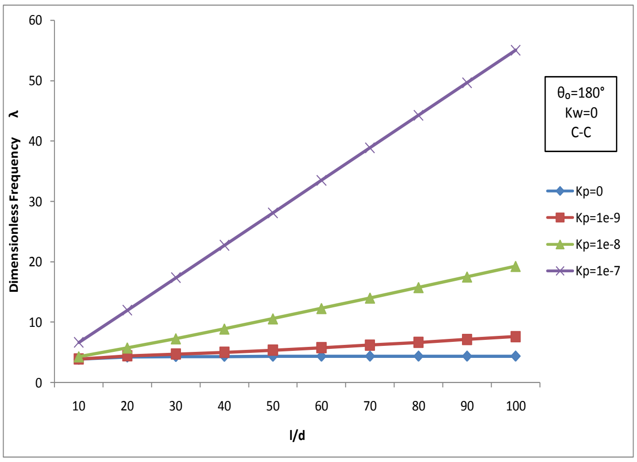

Figure 6: The effect of the Winkler foundation parameter with various slenderness ratios on the dimensionless frequencies of a circular SWCNT.

In figure 7, the effects of Pasternak and Winkler constants (K_P and K_W) on resonant frequency of a curved SWCNT are presented. In this situation, variations of the frequencies are inconsiderable when Pasternak coefficient and Winkler constant are less than 10^{-7} and 10^{7} respectively and with increasing in Winkler constant K_W the slope of the curves increase significantly. In this condition when Pasternak parameter K_P is equal to 10^{-5} the resonant frequency remains almost constant without any changes. This means that the stiffness of the medium due to the Pasternak-type model, in this case, is relatively large respect to the mass and the inertial effects of SWCNT.

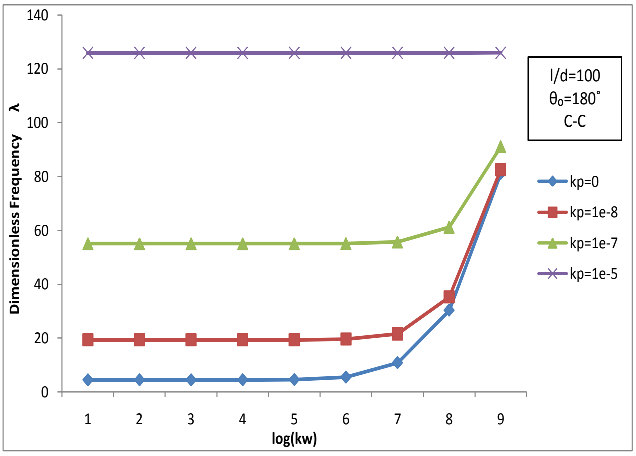

Figure 7: The effects of Pasternak and Winkler constants on the dimensionless frequencies of a circular SWCNT.

The effect of the boundary stiffness for the curved SWCNT with large and small aspect ratios on the frequency of in-plane vibration is shown in figure 8. In this case, it is supposed that the spring constants in the left and the right sides of the model have the same quantity ($K_{ta} = K_{tb} = K_{ra} = K_{rb} = C$).

The parameter C changes from 10^{-20} to 10^{35} and consequently, the boundary conditions of the curved SWCNT will vary from free-free to clamped-clamped boundary conditions. The variation of the natural frequencies as a function of supported end conditions for SWCNTs with large and small aspect ratios is revealed clearly. The figure indicates that when C is very small, the natural frequencies for nanotube with *l/d=10* and *l/d=100* are almost the same. While by increasing the stiffness of the ends, the natural frequency for SWCNT with a large aspect ratio will take higher values respect to the one with small *l/d*.

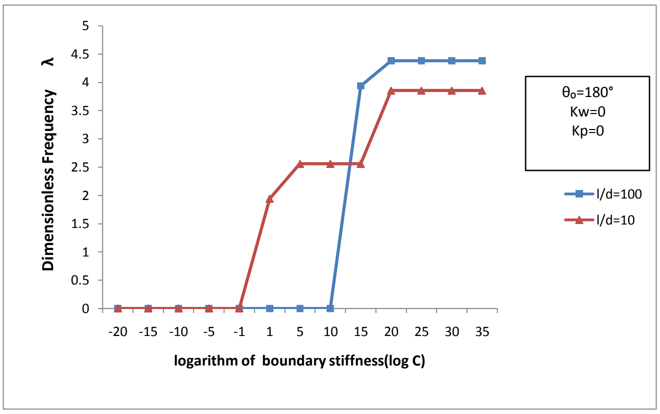

Figure 8: The effect of boundary stiffness on the dimensionless frequencies of a circular SWCNT.

Conclusions

The GDQR was applied to compute the natural frequencies for in-plane vibration of circular SWCNT in an elastic Winkler-type and Pasternak-type foundation under general boundary conditions. Timoshenko beam theory has been used in which both rotary inertia and shear deformation are taken into account. The results confirm that the resonant frequencies of a curved SWCNT are completely related to the stiffness of the elastic medium, modulus of the shear layer, slenderness ratio, and opening angle. The present approach is shown that the effects of the opening angle, the stiffness and the shear layer constants of the medium on the resonant frequency are perfectly significant when curved SWCNT has large aspect ratios.

References

[1] S. IJIMA, 1991, Helical microtubules of graphitic carbon, *Nature*, 56-58.

[2] J. Bernholc, C. Brabec, M.B. Nardelli, A. Maiti, C Roland and Yakobson BI, 1998, Theory of growth and mechanical properties of nanotubes, *Applied Physics A—Materials Science and Processing* 67 39–46.

[3] M.M.J. Treacy, T,W, Ebbesen and J.M. Gibson, 1996, Exceptionally high Young's modulus observed for individual carbon nanotubes, *Nature* 381, pp. 678–680.

[4] M.F. Yu, O. Lourie, M.J. Dyer, K. Moloni, T.F. Kelly and R.S. Ruoff, 2000, Strength and breaking mechanism of multiwalled carbon nanotubes under tensile load, *Science*, 287, pp. 637–640.

[5] R.H. Baughman, 1999, Carbon nanotubes actuators, *Science,* 284 , pp.1340–1344.

[6] H. Dai, J.H. Hafner, A.G. Rinzler, D.T. Colbert and R.E, Smalley, 1996, Nanotubes as nanoprobes in scanning probe microscopy, *Nature*, 384, pp. 50-147.

[7] W. Yang, X.L. Ma, H.T. Wang and W. Hong, 2003, The advancement of nanomechanics (continued), *The Advancement of Mechanics*, 33, pp. 175 –185.

[8] D. Qian, E.C. Dicky, R. Andrew and T. Rantell, 2000, Load transfer and deformation mechanisms in carbon nanotubes-polystyrene composites, *Applied Physics Letters,* 76(20), pp.2868-2871.

[9] A. Pantano, M.C. Boyce and D.M. Parks, 2003, Nonlinear structural mechanics based modeling of carbon nanotube deformation, *Physical Review Letters,* 91 (14), pp. 145501-1–145501-4

[10] R.D. Bradshaw, F.T. fisher and L.C. Brinson, 2003, Fiber waviness in nanotube-reinforced polymer-composites-II: modeling via numerical approximation of the dilute strain concentration tensor, *Composites Science and Technology,* pp. 1705-1722.

[11] R.F. Gibson and V. Anumandla, 2006, A comprehensive closed form micromechanics model for estimating elastic modulus of nanotube reinforced composites, *Composites: Part A*, pp. 2178-2185.

[12] N. Fathi Mayoof, M.A Hawwa, 2009, Chaotic behavior of a curved carbon nanotube under harmonic excitation, *Chaos, Solitons and Fractals*, 42, pp. 1860–1867.

[13] R.F. Gibson, O.A. Emmanuel and W. Yuan-Feng, 2007, Vibrations of carbon nanotubes and their, *composites: A review Composites Science and Technology,* pp. 67 1-28.

[14] R. Davis, R.D. Henshell and G.B. Warburton, 1972, Constant curvature beam finite elements for in-plane vibration Journal of sound and vibration, 25(4), pp. 561-576.

[15] W.B. Bickford and B.T. Strom, 1975, Vibration of plane curved beams Journal of sound and vibration, 39(2), pp. 135-146.

[16] T Irie, G Yamanda and K Tanaka, 1983, Natural frequencies of in-plane vibration of arcs, *Journal of applied mechanics*, 50, pp. 449-452.

[17] M.S. ISSA, T.M. WANG and B.T. HSIAO, 1987, Extensional vibrations of continuous circular curved beams with rotary inertia and shear deformation Free vibration, *Journal of Sound and Vibration*, 114(2), pp. 297-308.

[18] K. Kang, C.W. Bert and A.G. Striz, 1995, Vibration analysis of shear deformable circular arches by the differntial quadrature method, *Journal of sound and vibration*, 181(2), pp. 353-360.

[19] Y.P. Tseng, C.S. Huang and C.J. Lin, 1997, Dynamic stiffness analysis for in-plane vibrations of arches with variable curvature, *Journal of sound and vibration*, 207(1), pp. 15-31.

[20] V. Yildrim, 1997, A computer program for the free vibration analysis of elastic arcs, *Computers & Structures*, 62 (3), pp. 475-485.

[21] T. Murmu and S.C. Pradhan, 2009, Buckling analysis of a single-walled carbon nanotube embedded in an elastic medium based on nonlocal elasticity and Timoshenko beam theory and using DQM, *Physica E*, 41, pp.1232–1239.

[22] Z. Zong and Y. Zhang, 2009, Advanced Differential Quadrature Methods, *CRC Press*

[23] C.M. Wang, V.B.C. Tanb and Y.Y. Zhang, 2006, Timoshenko beam model for vibration analysis of multi-walled carbon nanotubes, *Journal of Sound and Vibration*, 294, pp. 1060–1072